

BEAM-BASED IMPEDANCE CHARACTERIZATION OF THE ALBA PINGER MAGNET

U. Iriso, T.F. Günzel, ALBA-CELLS, Cerdanyola de Vallès, Spain
 E. Koukovini-Platia, H. Bartosik, G. Rumolo, CERN, Geneva, Switzerland

Abstract

The ALBA pinger magnet consists on two short kickers (for horizontal and vertical planes) installed in a single Titanium coated ceramic vacuum chamber. Single bunch measurements in the vertical plane were performed in the ALBA Synchrotron Light Source before and after the pinger installation, and by comparing the Transverse Mode Coupling Instability (TMCI) thresholds for zero chromaticity, we infer the pinger impedance and compare it with the model predictions.

INTRODUCTION

Coupling impedance calculations are a key issue when designing an accelerator, in particular for electron light sources, where the presence of numerous Insertion Devices (IDs) with very small gaps can limit the circulating beam intensity in the machine. Often, these IDs are not made of a single material, but they are composed of different materials in different layers. Therefore, it is important to evaluate the reliability of the computer codes that evaluate the impedance of these devices before their installation.

At ALBA, a pinger magnet has been installed during the summer shutdown of 2014 [1]. The pinger magnet is a multi-layer structure composed by a ceramic vacuum chamber of 6.5 mm thickness, with an inner Titanium (Ti) coating of only 400 nm. This vacuum chamber is surrounded with a ferrite yoke [1], and between the ceramic and the ferrite there is a gap of 1 mm width for air cooling. This structure is exactly the same as the one used for the four injection kickers installed since day-1, with the only difference in the ferrite thickness surrounding the ceramic chambers [2].



Figure 1: Vertical (left) and horizontal (right) pinger magnet installed at ALBA during summer 2014. The ceramic chamber (in white) is visible between the two structures used for the vertical (left) and horizontal (right) excitations.

Figure 1 shows a picture of the pinger magnet, where the ceramic chamber is visible in the middle. The same vac-

uum chamber (780 mm in length) is used for the horizontal (left) and vertical kick excitations (right). The difference for each structure consists in the position of the Copper (Cu) electrodes, which are located on left/right for the horizontal excitation, and top/bottom for the vertical.

The goal of these studies is to infer the pinger magnet impedance based on beam measurements and compare it with results using different computer simulation codes (GdfidL, CST, and IW2D [3–5]). Beam-based impedance characterization of the pinger magnet are based on Transverse Mode Coupling Instability (TMCI) studies: by analysing the machine detuning and instability thresholds before the pinger installation (Autumn 2013) and after (Autumn 2014) we can infer the contribution of the new installed element to the total machine impedance.

BEAM-BASED MEASUREMENTS

TMCI Theory

Assuming a Gaussian beam bunch with N_b particles and rms length of σ_τ , the complex frequency shift in betatron frequency for the $l = 0$ mode is expressed by [6]

$$\Omega - \omega_\beta = -iZ_{\text{eff}} \frac{N_b e c^2}{4\sqrt{\pi}(E/e)T_0\omega_\beta\sigma_\tau}, \quad (1)$$

where $\omega_\beta = Q_\beta\omega_0$ the angular betatron frequency, Q_β is the betatron tune (including the integer part), ω_0 is the angular revolution frequency, E is the beam energy, c is the speed of light, and e the electron charge. The term Z_{eff} is the effective impedance of the machine, defined as:

$$Z_{\text{eff}} = \frac{\sum \beta_i Z_i}{\langle \beta \rangle}, \quad (2)$$

where Z_i , β_i refers to the impedance and beta function of the machine element i , respectively. Equation 1 shows that the imaginary part of Z_{eff} causes a tune shift with increasing bunch current, which allows to infer the total machine impedance, as already performed in other machines [6–8].

While the vertical detuning is proportional to $\text{Im}(Z_{\text{eff}})$, the threshold at which the instability occurs decreases with increasing the impedance (approximately like $1/Z_{\text{eff}}$). In general, there is no readily available formula relating the intensity threshold and the impedance, and this has to be inferred using computer simulation codes including bunch lengthening effects.

In the following, we focus our studies on the vertical plane because the pinger transverse aperture is 80×24 mm (horizontal \times vertical), and thus the effect is much more critical in the vertical plane.

TMCI Observations

The TMCI phenomenology is well observed on the tune monitor upon increasing the bunch current. Figure 2 compares the measurements taken (with In-Vacuum Undulators (IVUs) closed) during 2013 (blue) and during 2014 (red). In both cases, the chromaticity in the vertical plane was set as close as possible to 0 and the same rf voltage (2.1 MV) was used to keep the same synchrotron tune.

The measurements were taken in steps of about 1 mA, when the injection was halted to perform both tune and bunch length measurements. For an easy comparison, we plot the vertical tune shift with respect to the zero-current tune, normalized to the synchrotron tune Q_s . It is observed that the slope becomes steeper by 3.6% after the pinger's installation. The error bar in the data points stems from the statistical tune measurement fluctuation.

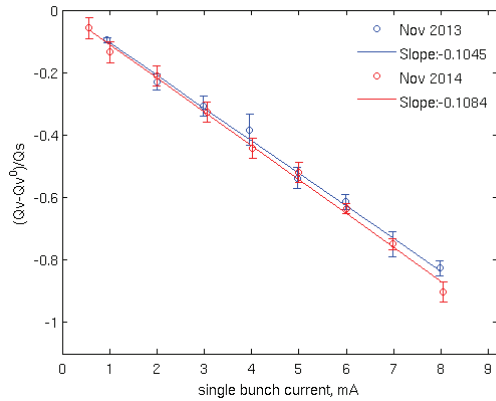


Figure 2: Comparison of the vertical detuning before (blue) and after (red) the pinger installation. The difference between the slopes in 2013 and 2014 is 3.6%.

Close to the instability threshold, the tune was recorded at every injection until the TMCI instability sets in. This is shown in Fig. 3, where it can be seen that when the instability is reached, partial beam loss occurs and the tune increases. The plot also shows that $I_{th} = 8.95$ mA during the measurements without the pinger magnet as already presented in Ref. [9], while after the pinger's installation the threshold reduces (as expected) to 8.45 mA, which corresponds to a difference of 4.5%.

During the measurements, we noticed that the TMC-Instability is sensible to several machine parameters, like rf voltage, bunch length, position of movable objects (like scrapers or IVUs), and chromaticity. In particular, precise control of the latter is complex. Considering all these factors, we conclude that the introduction of the pinger magnet (and its corresponding transition elements) has increased the ALBA impedance by $(4 \pm 1)\%$.

5: Beam Dynamics and EM Fields

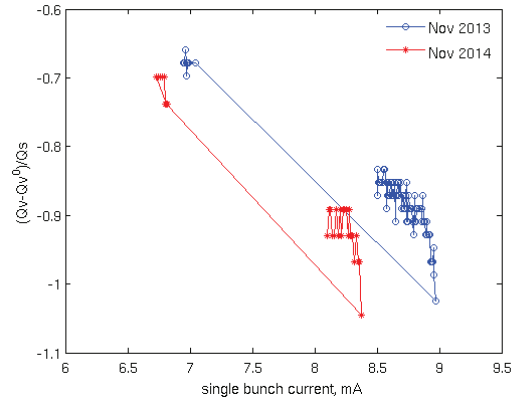


Figure 3: Injection from a bunch intensity close to the instability onset. We can see that the instability produces a partial beam loss, which in turn reduces the tune to a lower value. For the 2013 case, the instability threshold is found at 8.95 mA, while in 2014 the threshold is reduced to 8.45 mA.

Effective Impedance

From Eq. 1, the imaginary part of the effective impedance is estimated from the measured tune shift as:

$$\text{Im}(Z_{\text{eff}}) = \frac{dQ}{dI_B} 4\sqrt{\pi}(E/e)\omega_0\sigma_\tau \frac{1}{\langle\beta\rangle}, \quad (3)$$

where I_B is the bunch current. The precision of this measurement is also limited by the precision given by the bunch length measurement given by the streak camera, which we estimate at 10%.

Considering a bunch length of $\sigma_\tau = 20$ ps [10], the estimate before the pinger magnet's installation is $\text{Im}(Z_{\text{eff}}^{2013}) = 216$ k Ω /m, and it increases to $\text{Im}(Z_{\text{eff}}^{2014}) = 224$ k Ω /m after its installation in 2014. This is consistent with the results shown in Ref. [10], where thorough studies show not only measurements at 2.1 MV, but for different rf voltages (and thus varying the bunch length).

The pinger impedance is obtained from the difference between the two values, normalized by the ratio of $\langle\beta\rangle/\beta_p$, being β_p the local beta-function at the pinger. We obtain $\text{Im}(Z_{\text{eff}}^p) = (14.5 \pm 4)$ k Ω /m.

RESULTS FROM SIMULATION CODES

Model Prediction with IW2D

The impedance of the pinger magnet is estimated using an analytical code, ImpedanceWake2D [5], which is based on the exact solution of Maxwell equations. The code assumes long structures and flat geometries to model the magnet. Consistent with the pinger geometry, we simulate the pinger magnet with a 4-layer structure composed of a 6.5 mm thickness ceramic chamber with the 0.4 μm Ti coating, plus the external ferrite yoke. Between the ceramic and the ferrites, we also take into account the 1 mm thick layer of air required for air cooling. The material properties of the 4-layer structure are shown in Table 1.

Table 1: Material properties of the flat multilayer structure with ImpedanceWake2D.

Layers	σ (S/m)	$\epsilon' / \mu_r / f_{rel}$ (MHz)	d (mm)
1: Ti	2.38×10^6	1 / 1 / Infinity	4×10^{-4}
2: Ce	1×10^{-12}	9.3 / 1 / Infinity	6.5
3: Air	5×10^{-17}	1 / 1 / Infinity	1
4: Fe	1×10^{-4}	12 / 460 / 20	55

The simulated generalized vertical impedance for a 4-layer flat structure is shown in Fig. 4, comparing the real and the absolute value of the imaginary impedance for 0.1 and for 0.4 μm Ti coating. From the imaginary part of the computed impedance, the effective impedance for a Gaussian bunch can be calculated [6].

For a 0.4 μm thick Ti coating, the computed imaginary effective impedance, $\text{Im}(Z_{\text{eff}})$, is between 1.97-3.2 $\text{k}\Omega/\text{m}$, taking into account the observed bunch lengthening [9]. In order to obtain a value close to the measured one, the Ti coating would need to be reduced by a factor 4 (from 0.4 μm to 0.1 μm , see Fig. 4). However, according to resistance measurements along the pinger magnet, the Ti thickness varies between 0.36 and 0.402 μm , far from the 0.1 μm thickness required to produce the beam-based impedance measurement. The surface roughness and inhomogeneity of the coating are not taken into account. It is worth mentioning that other approaches give similar results [11].

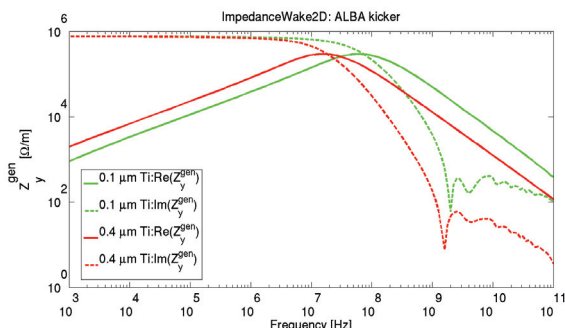


Figure 4: Vertical generalized impedance of the pinger magnet. In red, the Ti thickness assumed is 0.4 μm . In green, a thinner coating is considered of 0.1 μm .

Therefore, the measured effect of the pinger impedance seems to exceed by ~ 4 the model expectations. More detailed studies about the simulations using IW2D for the ALBA pinger and injector kickers are shown in Ref. [12].

Model Prediction with GdfidL

In order to complement the impedance from the surrounding material structure with the contribution from the cross section variation of the beam pipe, GdfidL calculations are carried out. Taking also the surrounding vacuum elements into account, we found a total geometrical contribution of only 0.85 $\text{k}\Omega/\text{m}$ (see Fig. 5).

Adding up geometrical and wall impedance contribution, a vertical impedance of 2.92 $\text{k}\Omega/\text{m}$ is obtained. An overview of all contributions is shown in Table 2.

Table 2: Impedance of the pinger magnet from the different contributions. The total impedance is 2.92 $\text{k}\Omega/\text{m}$ (@22 ps).

contribution	$\text{Im}(Z^P)$, $\text{k}\Omega/\text{m}$
dipolar broadband	0.64
quadrupolar broadband	0.21
dipolar RW	1.35
quadrupolar RW	0.71

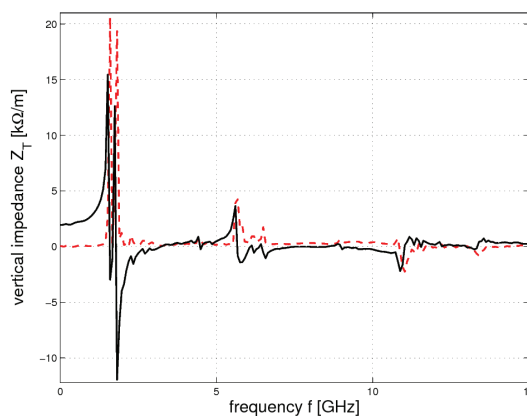


Figure 5: Real (red dashed line) and imaginary part (black) of the BBI impedance (dipolar part) computed with GdfidL.

CONCLUSION

The effective impedance produced by the pinger magnet has been measured by analyzing the TMCI detuning slopes and intensity thresholds before and after its installation. We evaluate $\text{Im}(Z_{\text{eff}}) = (14.5 \pm 4) \text{ k}\Omega/\text{m}$. The large (around 30% error bar) stems from the influence of the experimental machine settings in the TMCI measurements and the tune measurement spread.

On the other hand, computer simulation codes like IW2D and GdfidL provide an impedance of $\sim 3 \text{ k}\Omega/\text{m}$, which is almost a factor 4 smaller from the measured one. The difference is not understood and is currently under investigation. Several factors are under study, like the influence of the adjacent structures (tapers, bellows, etc), and the exchange of a dipole chamber for an infrared beamline.

In [10], good agreement is found regarding other multilayer structures (in-vacuum undulators) after careful cross-check of the surrounding structures. Therefore, we will not only look at the *room-for-improvement* in the computer simulation codes, but also to a more careful analysis of the pinger surrounding structures, as well as to the experimental machine set-up and bunch length parametrisation.

Content from this work may be used under the terms of the CC BY 3.0 licence (© 2015). Any distribution of this work must maintain attribution to the author(s), title of the work, publisher, and DOI.

REFERENCES

- [1] M. Pont et al. *A pinger magnet system for ALBA*, in these Proceedings.
- [2] M. Pont, R. Nunez, E. Huttel. WEPO013, IPAC11, San Sebastián, Spain.
- [3] W. Bruns, GdfidL, www.GdfidL.de
- [4] CST Microwave Studio- Getting Started (2003).
- [5] N. Mounet. *ImpedanceWake2D manual*.
http://impedance.web.cern.ch/impedance/Codes/Impedance-Wake2D/user_manual_todate.txt
- [6] A. W. Chao. *Physics of collective beam instabilities in high energy accelerators*. New York: Wiley, 1993.
- [7] R. Dowd et al, *Single bunch studies at the Australian Synchrotron*, Proc. of EPAC08.
- [8] A.-S. Müller et al, *Studies of current dependent effects at ANKA*, Proc. of EPAC04.
- [9] T.F. Günzel, U. Iriso, F. Perez, E. Koukovini-Platia, G. Rumolo. TUPRI052, IPAC14, Dresden, Germany.
- [10] T. Günzel et al, *Impedance Model Studies for the Interpretation of the Single Bunch Measurements at ALBA*, in these Proceedings.
- [11] V. Danilov, S. Henderson, A. Burov, V. Lebedev, An estimate of the SNS ring injection magnet coating impedance, EPAC'02, Paris, pp.1464.
- [12] E. Koukovini Platia. High frequency effects of impedances and coatings in the CLIC damping rings. CERN-THESIS-2015, to be published.